

UC San Diego

UC San Diego Previously Published Works

Title

Spinal parenchymal occupation by neural stem cells after subpial delivery in adult immunodeficient rats

Permalink

<https://escholarship.org/uc/item/0vm3t5g5>

Journal

Stem Cells Translational Medicine, 9(2)

ISSN

2157-6564

Authors

Marsala, Martin

Kamizato, Kota

Tadokoro, Takahiro

et al.

Publication Date

2020-02-01


DOI

10.1002/sctm.19-0156

Peer reviewed

**ENABLING TECHNOLOGIES FOR
CELL-BASED CLINICAL TRANSLATION**

Spinal parenchymal occupation by neural stem cells after subpial delivery in adult immunodeficient rats

Martin Marsala¹  | Kota Kamizato^{1,2} | Takahiro Tadokoro^{1,2} | Michael Navarro¹ | Stefan Juhas³ | Jana Juhasova³ | Silvia Marsala¹ | Hana Studenovska⁴ | Vladimir Proks⁴ | Tom Hazel⁵ | Karl Johe⁵  | Manabu Kakinohana² | Shawn Driscoll⁶ | Thomas Glenn⁶ | Samuel Pfaff⁶ | Joseph Ciacci⁷

¹Neuroregeneration Laboratory, Department of Anesthesiology, University of California, San Diego, La Jolla, California

²Department of Anesthesia, University of Ryukyus, Okinawa, Japan

³Institute of Animal Physiology and Genetics, Czech Academy of Sciences, Libechov, Czech Republic

⁴Department of Biomaterials and Bioanalogous Systems, Institute of Macromolecular Chemistry, Czech Academy of Sciences, Prague, Czech Republic

⁵Neuralstem Inc., Germantown, Maryland

⁶Gene Expression Laboratory, Howard Hughes Medical Institute, Salk Institute for Biological Studies, La Jolla, California

⁷Department of Neurosurgery, University of California, San Diego, La Jolla, California

Correspondence

Martin Marsala, MD, Department of Anesthesiology, Sanford Consortium for Regenerative Medicine, 2880 Torrey Pines Scenic Drive, La Jolla, CA 92037.
Email: mmarsala@ucsd.edu

Funding information

Czech Ministry of Education, Youth and Sports, Grant/Award Number: LO1609; NIH, Grant/Award Numbers: NS047101, R01OD018272

Abstract

Neural precursor cells (NSCs) hold great potential to treat a variety of neurodegenerative diseases and injuries to the spinal cord. However, current delivery techniques require an invasive approach in which an injection needle is advanced into the spinal parenchyma to deliver cells of interest. As such, this approach is associated with an inherent risk of spinal injury, as well as a limited delivery of cells into multiple spinal segments. Here, we characterize the use of a novel cell delivery technique that employs single bolus cell injections into the spinal subpial space. In immunodeficient rats, two subpial injections of human NSCs were performed in the cervical and lumbar spinal cord, respectively. The survival, distribution, and phenotype of transplanted cells were assessed 6–8 months after injection. Immunofluorescence staining and mRNA sequencing analysis demonstrated a near-complete occupation of the spinal cord by injected cells, in which transplanted human NSCs (hNSCs) preferentially acquired glial phenotypes, expressing oligodendrocyte (Olig2, APC) or astrocyte (GFAP) markers. In the outermost layer of the spinal cord, injected hNSCs differentiated into glia limitans-forming astrocytes and expressed human-specific superoxide dismutase and laminin. All animals showed normal neurological function for the duration of the analysis. These data show that the subpial cell delivery technique is highly effective in populating the entire spinal cord with injected NSCs, and has a potential for clinical use in cell replacement therapies for the treatment of ALS, multiple sclerosis, or spinal cord injury.

KEYWORDS

glia limitans formation from grafted neural precursors, human-specific mRNA sequencing, immunodeficient rat, neuraxial neural precursor migration, subpial stem cell injection

1 | BACKGROUND

The use of spinally targeted cell-replacement therapies for the treatment of a variety of neurodegenerative disorders, including amyotrophic lateral sclerosis (ALS) and spinal cord injury (SCI), has recently reached the

clinical trial stage with several phase I or phase II trials underway. Extensive preclinical studies in rodent and large animal models of ALS and SCI have tested several spinal cell delivery techniques to define the most effective and safe cell delivery approach to be used in human clinical trials.

This is an open access article under the terms of the Creative Commons Attribution-NonCommercial-NoDerivs License, which permits use and distribution in any medium, provided the original work is properly cited, the use is non-commercial and no modifications or adaptations are made.

© 2019 The Authors. STEM CELLS TRANSLATIONAL MEDICINE published by Wiley Periodicals, Inc. on behalf of AlphaMed Press

A direct parenchymal injection of cells is the most frequently used technique and was successfully used in both rodent and large animal models.¹⁻⁶ In some of these studies, a statistically significant neuroprotective effect (as defined by the recovery of motor function and decreased neuronal degeneration) was demonstrated providing a rationale for further preclinical development of cell-replacement therapies for ALS and SCI.^{2,3,5,6} An intrathecal cell delivery was also used to test the treatment potency of neural precursors in rat spinal trauma model.⁷

In recently completed and ongoing clinical trials, an invasive cell delivery technique that requires direct needle penetration into the spinal parenchyma is used to deposit cells into the specific spinal target (such as the ventral horn gray matter).⁸⁻¹⁰ Although effective in delivering cells into the spinal parenchyma, the invasive nature of this approach limits the number of injections that can be performed. Accordingly, this cell-delivery approach is not effective in achieving trans-spinal occupation by grafted cells. This limitation can be of significant importance, particularly in the treatment of spinal neurodegenerative diseases characterized by multisegmental degeneration (such as spinal traumatic injury) or pan-neuronal degeneration (as seen in inherited or sporadic forms of ALS). Because of safety concerns, the current clinical protocols for cell delivery only employ regional cell injections (cervical and lumbar enlargements in ALS) or peri-injury injections (in case of spinal trauma).

In a recently completed phase II dose-escalation ALS trial, a maximum of 20 cell injections of human fetal neural precursor cells (hNSCs) (NSI-566) were delivered at lumbar and cervical levels of the spinal cord.⁹ The highest total cell dose delivered in a single patient was 16 million, and covered a region of approximately 8 cm length. Considering the length of the spinal cord in adult humans is approximately 50 cm, this 8 cm region represents only a portion of spinal cord gray matter mass which can potentially benefit from regional cell replacement therapy. In an ongoing phase I trial for the treatment of chronic SCI with spinal injections of fetal hNSCs, a total of six injections are being delivered around the injury epicenter (10 μ l each, 200 000 cells/injection).¹¹ In a second completed phase I subacute spinal trauma trial, human embryonic stem cell-derived oligodendrocyte precursors (AST-OPC1) were injected (2 million cells) at a single site 5 mm caudal to the injury epicenter. In another ongoing AST-OPC1 dose-escalation study, the maximum cell dose planned is 20 million cells delivered as a single injection.¹⁰ The primary rationale for using OPCs as a cell-based therapeutic in spinal trauma is to accelerate local remyelination and promote/restore axonal conductivity. It is expected that the ability to achieve rapid and multisegmental delivery of OPCs will likely be associated with a more pronounced therapeutic effect.

As described, the use of a limited number of direct parenchymal cell injections represents a key limiting factor in achieving multisegmental cell repopulation in spinal cord treatment protocols. Accordingly, the development of a safer and more effective spinal cell delivery technique to achieve rapid and multisegmental spinal cord repopulation by injected cells would represent a significant improvement over the currently available protocols.

Recently, we have described a novel subpial AAV9 delivery technique and demonstrated robust multisegmental transgene expression in adult pigs, rats, and mice.^{12,13} We have also demonstrated that the pia

Significance statement

This article describes a novel subpial spinal cell delivery technique that does not require direct spinal tissue needle penetration and is associated with robust spinal cord occupation by subpially injected cells. The effectiveness of this cell delivery technique was validated in long-term studies in immunodeficient rats receiving subpial injection of human neural precursors. This is the first report to demonstrate the successful spinal cell occupation by neural stem cells, which do not require invasive central nervous system or spinal cord cell delivery. Because of the simplicity of this approach, the use of this technique can substantially improve current clinical protocols aimed at spinal delivery of therapeutic cells in the treatment of spinal neurodegenerative disorders.

mater represents the primary barrier that limits vector penetration into the deep spinal parenchyma. To our knowledge, the use of the subpial space as a potential route for spinal cell delivery has not been explored. In our current study, we analyzed the survival, rostrocaudal migration and differentiation profile (neuronal and glial differentiation) of hNSCs at 6-8 months after subpial delivery in immunodeficient rats. We demonstrate that spinal subpial injection leads to the near complete occupation of the entire rat spinal cord by injected hNSCs at 6-8 months after cell delivery. In addition, a recently developed human-specific mRNA sequencing protocol that differentiates human from rat transcripts was used to characterize the gene expression profile of subpially injected hNSCs. No neurologically defined side effects (motor or sensory) or tumor formation was seen in any animal. These results represent a significant advance in the effort to develop a more efficient cell-delivery system for the treatment of spinal cord neurodegenerative disorders.

2 | METHODS

All procedures were approved by the Institutional Animal Care and Use Committee by the University of California, San Diego (Protocol No.: S01193). All studies were performed in such a manner as to minimize group size and animal suffering. Adult Sprague-Dawley immunodeficient rats (CrI:NIH-Foxn1^{rmu}; Charles River) male and female, 250-350 g; ($n = 6$) were used in this study.

2.1 | Placement of subpial cell-injection needle

Rats were anesthetized with 5% isoflurane and maintained at 2%-3% isoflurane during surgery depending on breathing rate and paw pinch response. The back of the rat was then shaved and cleaned with 2% chlorhexidine. After skin incision, the paravertebral muscle surrounding the cervical and lumbar spinal vertebrae was removed and animals were mounted into a spinal immobilization frame (Stoelting) using Cunningham's spinal clamps, as previously described.¹⁴ To expose the spinal cord, dorsal laminectomy of the C-C3 and Th11-L1 vertebrae

was performed using a dental drill. The dura was then cut open using a scalpel blade or 30G needle.

To inject cells into the subpial space, two sequential procedural steps that used two independent XYZ manipulators (Supporting Figure S1A,B) were used. From the time point of dura exposure, all subsequent manipulations were performed under a dissecting scope with $\times 5$ -10 magnification. First, a 33G pia-puncturing needle with the tip bent at 90° and mounted on the Z arm was used to puncture the pia (Figure S1C). The puncturing needle was previously sharpened using a glass capillary beveller (Pipet Micro Grinder EG-40; Narishige) with Diamond abrasive plate—coarse (5.0-50 μm tip sizes). After the pia was punctured, the puncturing needle was removed. In the majority of cases, the site of the punctured pia is easily recognizable even if the puncturing needle is removed. Second, a blunt 33G needle mounted on the second Z arm was then advanced into the subpial space through the pia opening. The needle was advanced into the subpial space for approximately 4-6 mm (Figure S1D,E). For demonstration purposes, contrast (Evans blue) was injected in the pilot experiment to demonstrate the spread of subpially injected solution. As shown in Figure S1F, a clear spread of contrasted solution in the ipsilateral subpial space can be seen immediately after injection.

2.2 | Source, preparation, and injection of hNSCs into the subpial space

The human cortical NSC lines (NSI-HK532) were provided by Neuralstem, Inc. (Germantown, Maryland, <http://www.neuralstem.com>). Briefly, HK532 were prepared from cortical tissue obtained from a single 8-week-old human fetus following an elective abortion, as previously described.¹⁵ The material was donated to Neuralstem, Inc. with informed consent in a manner compliant with guidelines of the National Institutes of Health and the FDA, and according to guidelines that were reviewed and approved by an outside independent review board.

Cells used for transplantation were harvested as an undifferentiated nestin-immunopositive population. In our current study, stably GFP-expressing cells prepared by lentiviral infection of HK532 line with HIV1-UBI-GFP vector were used. Previously cryopreserved cells were thawed, washed, and resuspended in hibernation media at a concentration of 80 000/ μl . Cells were delivered into the subpial space through the previously subpially placed 33G needle interconnected to a digital microinjector at a rate of 1 $\mu\text{l}/\text{s}$. A total of 20 μl of cell suspension was delivered at each C2-C3 and Th12-L1 subpial site in each animal (ie, total of 40 $\mu\text{l}/\text{animal}$; total of 3.2 million cells).

In order to analyze the differentiation of HK532 and HK-532-UBI-GFP *in vitro*, cells were grown to confluence and the media was changed to medium lacking growth factors to initiate differentiation.¹⁵ After 10 days, cells were fixed in 4% paraformaldehyde and immunostained using neuron-specific and glia-specific markers (see Immunofluorescence Staining; Table 1).

2.3 | Analysis of motor and sensory function

The effect of combined cervical and lumbar subpial cell delivery on neurological function was analyzed in all animals (6 rats) in 14-day

intervals for 6 months. Open field locomotion testing: changes in motor function was assessed using a Basso, Beattie, Bresnahan open field 21 grade locomotion rating scale.¹⁶ The presence of allodynia was tested by presence/absence of vocalization/withdrawal from touching the trunk around the level of subpial cell delivery with a 20 g von Frey filament.

2.4 | Perfusion fixation, postmortem *in situ* GFP fluorescence imaging, and immunofluorescence staining of spinal cord/brain sections and *in vitro*-induced hNSCs

At 6 months after cell delivery, rats were deeply anesthetized with pentobarbital and transcardially perfused with heparinized saline (200 ml) followed by 4% paraformaldehyde in PBS (250 ml-rats). The spinal cords and brains were then dissected and imaged *in situ* using Spectrum optical imaging system (Xenogen, Alameda, California). Sequences were acquired at excitation wavelength 465 nm and emission wavelength 520 nm. Medium binning was used, and the exposure time was 3 seconds. Images were analyzed using Living Image 4.3.1 (Xenogen) software. The signals were calculated using fixed volume region of interests (ROIs). After that, spinal cords and brains were cryoprotected in 30% sucrose PBS until transverse or longitudinal sections (30- μm -thick) were cut on a cryostat and stored in PBS. Sections were then stained with neuron-specific or glia-specific primary antibodies (Table 1) using the previously reported staining protocol.⁵ Then, staining sections were mounted on slides, dried at room temperature, and covered with a Prolong anti-fade kit (Invitrogen). *In vitro*-induced and 4% paraformaldehyde-fixed hNSCs were stained using neuron or glia-specific primary antibodies (Table 1).

Fluorescence images were captured using a Zeiss Imager M2 microscope and confocal images were taken using an Olympus FV1000 microscope.

2.5 | Quantification of subpially injected hNSCs

The total numbers of cells immunoreactive for hNUMA was estimated after counting the total number of hNUMA+ cells in transverse spinal cord sections taken from the cervical, thoracic, and lumbar spinal cord in rats ($n = 3$). Six sections (thickness of each section = 20 μm) taken from each spinal cord level were used for counting (ie, total 18 sections used per animal). The average number of counted cells calculated from 18 sections (ie, average number of cells in a single transverse 20- μm -thick section) was then multiplied by 4075 to estimate the total number of cells in the cervico-lumbar spinal cord (length of cervico-lumbar spinal cord = 8.15 cm/20 [μm] = 4075).

The percentage of Olig2, hGFAP, and Vimentin and Ki67+ cells relative to the total number of GFP+ cells was counted in 4 cervical and 4 lumbar transverse spinal cord sections in rats ($n = 3$). Double-labeled cells were counted separately in the white matter (dorsal, lateral, and ventral funiculi) and gray matter.

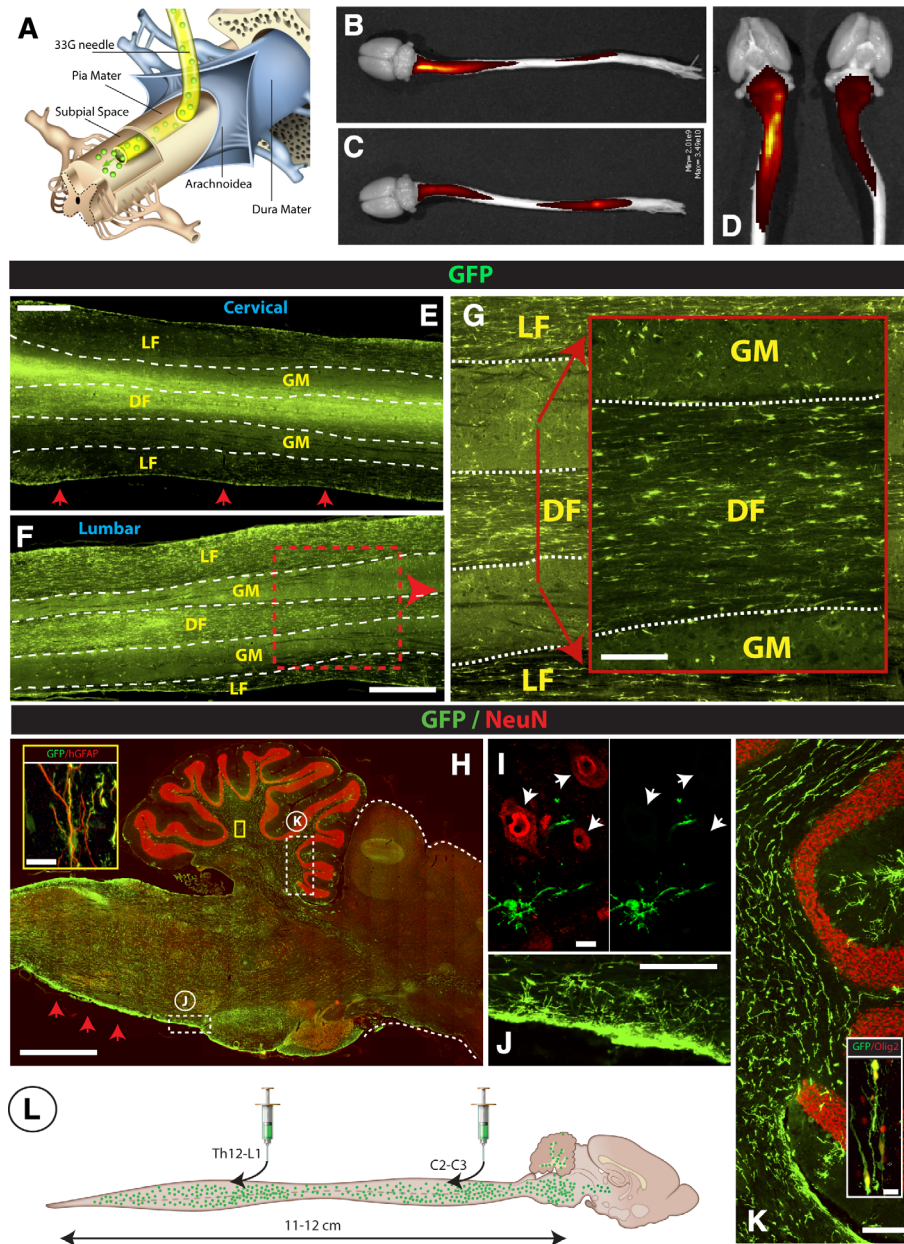


FIGURE 1 Spinal subpial injection of human GFP+ hNSCs leads to long-term injected-cell survival in the subpial space and intraparenchymal migration throughout the whole spinal cord, medulla, and white matter of the cerebellum in immunodeficient rats. A, Adult immunodeficient rats received a cervical and lumbar subpial injection of human fetal GFP+ hNSCs using a 33G subpial needle. At 6 months after cell delivery, animals were perfusion fixed, spinal cord and brain dissected, and imaged in situ using an IVIS Spectrum optical imaging system. After imaging, tissue was used for immunofluorescence staining of spinal cord and brain sections. B-D, Surface GFP fluorescence seen in two individual rats (B, C) shows an intense GFP signal on the dorsal cervical and lumbar spinal cord. Similar GFP fluorescence on the ventral cervical spinal cord can be seen in the same animals (D). E-G, A high density of GFP+ cells in the spinal cord parenchyma in horizontally cut spinal cord sections taken from the cervical (E) and lumbar (F) spinal cord can be identified. A relatively higher number GFP+ cells was seen in the white matter funiculi (LF, DF) if compared to gray matter (GM) (G). H-K, Analysis of sagittal brain sections shows a high density of injected GFP+ cells in the medulla oblongata, in the vicinity of glia limitans (H-red arrows; J) and the white matter tracts of the cerebellum (K). Similarly as seen in the spinal cord, the majority of GFP+ cells showed colocalization with Olig2 (K-inset) and GFAP (H-inset). 0.3 µm optical images showing no NeuN expression in injected GFP+ cells (I). L, Schematic drawing of spinal and brain GFP+ cell distribution at 6 months after cervical and lumbar subpial cell delivery. Scale bar: E, F, 1 mm; G, 150 µm; H, 2 mm; H-inset, 15 µm; I, 10 µm; J, 200 µm; K, 200 µm; K-inset, 15 µm, LF, DF-lateral, and dorsal white matter funiculi, GM, gray matter

2.6 | mRNA sequencing of human-specific transcripts in grafted rat spinal cord

Total RNA was isolated from flash frozen hNSC-grafted spinal cord and brain specimens using the Qiagen RNeasy Plus Mini kit. Approximately

1-2 µg of RNA was isolated from each sample, with RIN scores of ~9.0, as determined by TapeStation analysis (Agilent). SR75 mRNA sequencing libraries were prepared using the Illumina Stranded mRNA Library kit, and sequenced on the Illumina HiSeq4000 platform at the sequencing core at the UCSD IGM Genomics Center.

TABLE 1 Primary antibodies used for indirect immunofluorescence and histology

Catalog number	Name	Company
ab134970	Chicken-anti GFP 1:1000	Abcam
TA302094	Rabbit anti-GFAP (human specific) 1:1000	Origene, Rockville
C9205	Mouse anti-GFAP (Cy3-labeled) 1:500	Sigma-Aldrich
574597-1ml	Sheep anti-SOD1 1:500	Calbiochem, EMD Millipore
MAB377	Mouse anti-NeuN 1:1000	EMD Millipore
ABN78	Rabbit anti-NeuN 1:500	EMD Millipore
AB9610	Rabbit anti-Olig2 1:500	EMD Millipore
L8271	Mouse anti-Laminin 1:1000	Sigma-Aldrich
Ab11575	Rabbit anti-Laminin 1:500	Abcam
130-095-822	Mouse anti-GLAST 1:1000	Myltenyi Biotech
MAB1281	Mouse anti-NUMA (human specific)	EMD Millipore
AB6667	Rabbit anti-Ki67	Abcam
560341	Mouse anti-Nestin (Alexa Fluor 647-labeled) 1:500	BD Pharmingen
MAB5326	Mouse anti-Nestin (human specific) 1:500	EMD Millipore
18-0052	Mouse anti-Vimentin 1:1000	Zymed Laboratories
AB5733	Chicken anti-Vimentin 1:500	EMD Millipore
MAB5384	Mouse anti-NG2 1:500	EMD Millipore
AB5320	Rabbit anti-NG2 1:200	EMD Millipore
OP80-100UG	Mouse anti-APC	Oncogene

Single-end 75 bp reads (Illumina HiSeq4000) were received in FASTQ format and were prepared for downstream analysis by trimming known barcodes and then selecting post-trimmed reads for those with average base quality >15. Following the previously described preprocessing steps,¹⁷ reads were aligned with HISAT2 to a combined rat (Rn6) and human (Hg38) genome index. We used -k 20 and -score-min L,0,-0.4 with otherwise default settings. Aligned reads were sorted by read name and then evaluated for species of origin with an in-house perl script. The vast majority of reads only aligned to a single genome,

but for those that aligned to both genomes we used the HISAT2 alignment score to guide species assignment. If a read mapped equally well to both genomes then it was flagged as ambiguous and excluded from downstream analysis. Otherwise the read was assigned to the species for which it has the best alignment score.

Species assigned reads were quantified using Kallisto. Human reads were quantified against the full Gencode annotation (v28) and rat assigned reads were quantified against the Refgene annotation for the Rn6 genome (obtained from the UCSC Genome Browser). Kallisto “quant” was run in single-end mode with average fragment length of 200 and SD of 60. All downstream analysis was performed in R. Human and rat quantified expressions were combined into a single table and treated as a single-species for normalization. After calculating TPM scaled expression we split the human and rat gene-sample read count matrices apart for further analysis.

3 | RESULTS

3.1 | Subpially injected hNSCs survive, proliferate, and migrate throughout neuraxis

We first analyzed survival, migration, and differentiation of hNSCs when injected into the spinal subpial space. Adult immunodeficient rats received two bolus injections of hNSCs expressing GFP, one at cervical cord level (C3-C5) and another at lower thoracic-upper lumbar cord level (Th12-L1) in the dorsal subpial space (Figure 1A). Rats were perfusion-fixed 6 months later and the spinal cord and brain dissected and analyzed. First, the whole brain and spinal cord were scanned using an IVIS surface fluorescent scanner. Intense GFP fluorescence was seen in subpial space at the GFP+ cell-injected cervical and lumbar regions (Figure 1B,C). GFP signal was seen at both the dorsal (Figure 1B,C) as well as the ventral (Figure 1D) surface of the spinal cord, suggesting an effective spread of injected cells from the dorsal subpial space (ie, the site of subpial injections) into the ventral subpial compartment. Histological analysis of horizontally cut cervical and lumbar sections showed a widespread of GFP+ cells in the dorsal and lateral funiculi of white matter as well as the gray matter (Figure 1E,F). A higher proportion of GFP+ cells was seen in white matter as compared to gray matter in the same region (Figure 1G).

Analysis of sagittal brain sections showed extensive cell migration into the medulla oblongata, brain stem, and white matter tracts of the cerebellum (Figure 1H-K). Consistent with surface fluorescence scanning data, a higher density of injected cells was seen just below the pial surface in the dorsal, lateral, as well as ventral subpial compartments (Figure 1E,H, red arrows). Analysis of transversally cut sections showed the highest density of cells immunopositive for human-specific nuclear antigen (hNUMA), in segments that were near the injection sites. In those sections, cells were present in both the white and gray matter (Figure S3A,D). Quantitative analysis of the total number of hNUMA positive cells counted in the whole spinal cord from the upper cervical to the lower lumbar [C1 – L5] segments showed an estimated number of cells at $15\,650\,000 \pm 456\,000$ ($N = 3$). Compared to the injected number of cells (3.2 million), this represents approximately a 5.5-fold

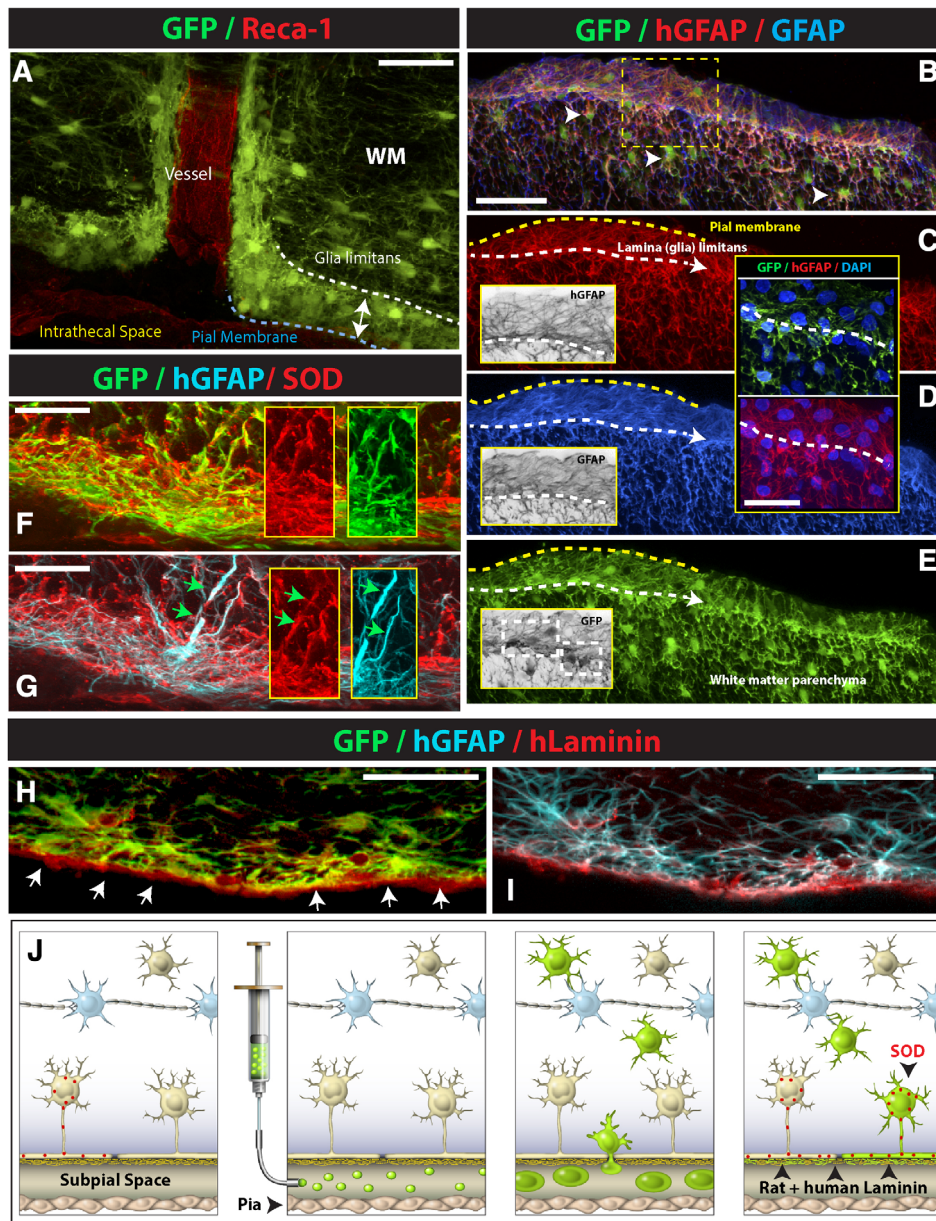


FIGURE 2 Subpially injected GFP + hNSCs accumulate in the vicinity of the superficial and vascular glia limitans and differentiate into astrocytes which functionally incorporate into the glia limitans. A, A multilayer of GFP+ cells can be seen in the subpial space, contributing to the formation of superficial and perivascular glia limitans. B-E, At the level of the glia limitans, injected human GFP+ hNSCs differentiate exclusively into human astrocytes (hGFAP) and extend foot processes which are similar to endogenous astrocyte-derived foot processes (compare BW insets in C, D, E). F-I, Injected glia limitans-forming human astrocytes express superoxide dismutase (SOD) (F, G) and synthesize extracellularly-deposited human-specific laminin (hLaminin) (H, I). J, Schematic drawing of postulated migration and functional maturation of subpially injected hNSCs in immunodeficient rats: after injection, cells start to migrate into the spinal parenchyma across the glia limitans. A subpopulation of cells differentiates into astrocytes, incorporate into glia limitans, and start to express functional markers characteristic of glia limitans-forming astrocytes, including SOD and laminin. The other population of injected cells continues to migrate into the spinal parenchyma, giving rise to parenchymal protoplasmic astrocytes and oligodendrocytes. Scale bars: A, 50 μ m; B, 60 μ m; C, D (inset), 30 μ m; F, G, 20 μ m; H, I, 50 μ m; WM, white matter)

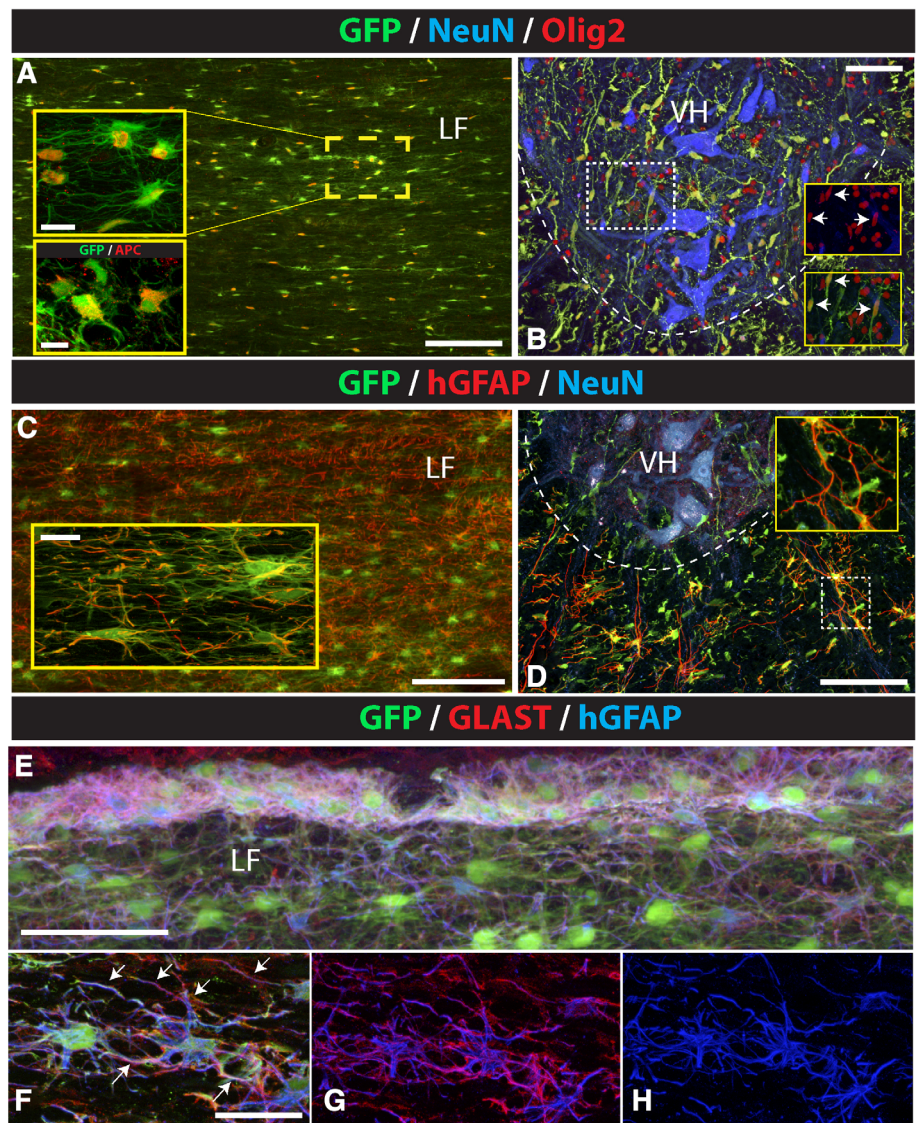
increase in the cell number after 6 months. Measurement of the distance of cell migration in the rostrocaudal neuraxis showed the presence of cells in the whole length of the spinal cord and extending up to the brain stem, that is, the total distance of approximately 12 cm achieved from one mid-cervical and one lower thoracic-upper lumbar subpial injection (Figure 1L). Quantitative analysis of hNUMA positive cells (depicted in S3A-F) in dorsal and ventral white and gray matter in cervical, thoracic and lumbar segments is presented in Figure S4A,B.

3.2 | Injected hNSCs-derived astrocytes mature and acquire morphological and phenotypic characteristic of glia limitans-forming endogenous astrocytes

Using higher power imaging and confocal microscopy, we next studied the detailed localization and phenotype of GFP+ cells. First, using

horizontally cut sections, a multilayer of GFP+ cells was consistently seen in the subpial space across multiple spinal segments rostral and caudal to the cell injection sites (Figure 2A,E). Similarly, co-staining with endothelial marker (Reca-1) showed a clear presence of GFP+ cells in the subpial-perivascular space (Figure 2A). Second, to probe for the contribution of the GFP+ cells to formation of glia limitans, sections were stained with human-specific and nonspecific (ie, cross-reacting with rat and human) anti-GFAP antibody. The glia limitans (also called glial limiting membrane or lamina limitans) is the outermost layer of spinal neural tissue and is composed of astrocytes and their foot processes. The primary function of the glia limitans is the prevention of the migration of neurons and neuroglia into the meninges and restriction of the entry of inflammatory cells and small molecules into the brain and spinal parenchyma.^{18,19} In the analyzed sections, numerous GFP+ cells were found (a) between the pia mater and glia limitans, (b) to be

FIGURE 3 Preferential astrocyte and oligodendrocyte differentiation of subpially injected hNSCs. A-D, Analysis of horizontal and transverse spinal cord section stained with GFP/Olig2, GFP/hGFAP, or triple-stained with GFP/NeuN/Olig2 and GFP/NeuN/hGFAP antibodies show a high density of Olig2-immunoreactive cells co-localizing with GFP in the white and gray matter in cervical segments (A, B). Staining with APC antibody shows expected cytoplasmic expression in GFP+ cells (A, lower inset). hGFAP expression was seen in astrocytes in the white matter but not in GFP+ cells in the gray matter (C, D). E-H, Co-staining of horizontal spinal cord sections with GFP/GLAST and hGFAP antibody showed that virtually all human astrocytes in the glia limitans as well as in the deeper white matter were GLAST positive. Scale bars: A, 150 μ m, A (insets), 15 μ m, 10 μ m; B, 100 μ m; C, 150 μ m, C (inset), 15 μ m; D, 100 μ m; E, 60 μ m; F, 30 μ m; LF, lateral funiculus; VH, ventral horn



integrated at the level of the glia limitans, and (c) below the glia limitans in deeper spinal white matter parenchyma (Figure 2B-E). By comparing the staining pattern of GFP+ cells between sections stained with human-specific vs nonspecific GFAP antibody, a very similar pattern was seen. This was characterized by the presence of GFP+ protoplasmic astrocytes in the deeper spinal white matter parenchyma (ie, below the glia limitans) (Figure 2B, white arrowheads) and surface glia limitans-forming GFP+ astrocytes with elaborate foot processes seen in the outermost layer of the spinal cord (compare Figure 2C vs D; B/W insets). These data show that, based on the morphological criteria, hNSC-derived astrocytes effectively populated the host glia limitans and acquired the morphological phenotype that appears to be identical to this specialized glia limitans-forming endogenous astrocytes.

One of the protective mechanisms of the glia limitans is its role in suppressing/modulating the effect of oxidative stress. Glia limitans-forming astrocytes have been reported to selectively express the superoxide dismutase (SOD).²⁰ SOD expression is not seen in parenchymal astrocytes.⁸ Therefore, we next tested if the hNSC-derived

astrocytes in the glia limitans also overexpressed SOD. As shown in Figure 2F,G, a high level of SOD expression was seen throughout the glia limitans with numerous GFP+ and human-specific GFAP-expressing astrocytes and their processes expressing the SOD.

Another protective mechanism associated with the function of glia limitans-forming astrocytes is its contribution to the formation of the parenchymal basal membrane by synthesis of laminin.²¹ We have therefore stained spinal cord sections with human-specific laminin (hLam) antibody and compared the staining pattern with sections stained with pan-laminin antibody (pLam) (ie, which cross-react with rat and human laminin). A specific surface-bound staining was seen after staining with hLam (Figure 2H,I) and this staining pattern was similar to the pLam staining pattern (Figure S5C-E).

Jointly, these data show that after subpial injections, hNSC-derived glial progenitors can survive in the subpial space long-term, incorporate into the glial limitans, as well as migrate deep into the spinal parenchyma. Terminally differentiated astrocytes homed in the glia limitans, acquire morphological characteristics that are consistent with

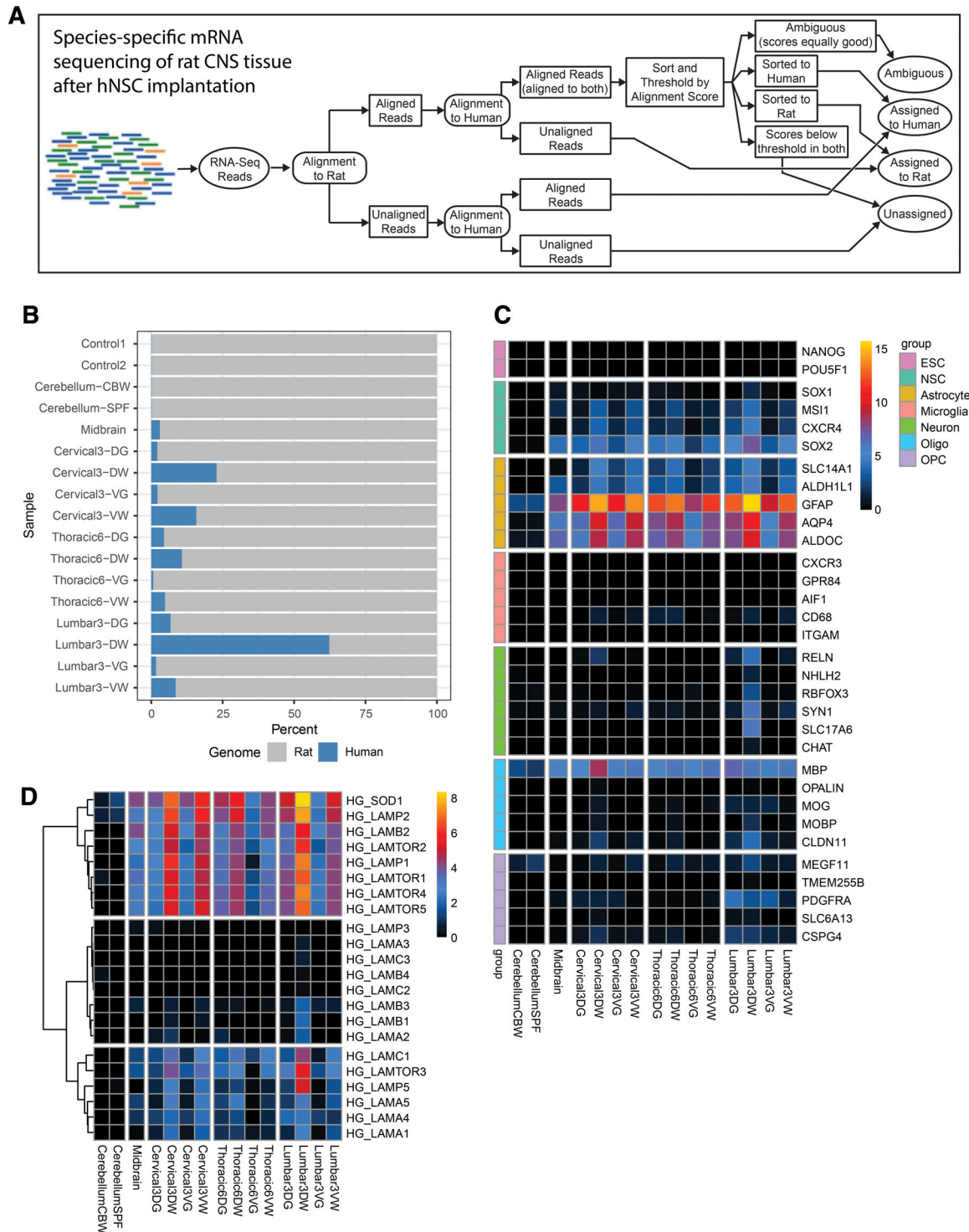


FIGURE 4 Species-specific mRNA sequencing analysis of hNSC-grafted tissue in immunodeficient rats at 8-months postinjection.

A, Schematic of the experimental design. mRNA sequencing reads were analyzed with a bioinformatics pipeline that assigns reads to species of origin (human or rat). **B**, Graph showing the percentage of human and rat transcripts among all of the samples tested. A significant percentage of human transcripts was detected in all tissue samples except for the cerebellum. **C**, Heat map demonstrating cell-type-specific human transcripts detected in grafted tissue. The cell-type-specific genes of interest are organized in groups corresponding to ESCs, NSCs, astrocytes, microglia, neurons, oligodendrocytes, and oligodendrocyte precursor cells (OPCs). Gene expression indicates that injected hNSCs differentiated into predominately astrocytes and oligodendrocyte lineage cells, with trace amounts of neurons. Additionally, there remains a significant number of NSC associated transcripts. ESC pluripotency genes did not show any enrichment. **D**, Expression profiles of human-specific laminin and SOD1 transcripts across all samples

TABLE 2 Quantitative analysis of GFAP, Olig2, Ki67, and vimentin-positive cells derived from subpially injected GFP+ human NPCs at 6 months post-subpial injection in rat

	GFP/Olig2	GFP/hGFAP	GFP/Ki67	GFP/vimentin
Gray matter	97.7 ± 4	0	0.82 ± 1.2	53 ± 5.4
White matter	69.4.0 ± 15	45 ± 10	1.1 ± 0.9	89 ± 4

Note: Data are expressed as percentage of double-stained GFP/Olig2, GFP/hGFAP, GFP/Ki67, and GFP/Vimentin cells relative to total number of GFP+ cells.

endogenous glia limitans-forming astrocytes and respond to a local function-guiding signals by synthesis of SOD- and spinal surface-bound laminin (Figure 2J).

3.3 | Subpially delivered hNPCs show preferential glial (astrocyte and oligodendrocyte) differentiation

We next analyzed the neuronal differentiation profile of the GFP+ cells by co-staining of horizontal or transverse spinal cord sections in rats with anti-neuronal (NeuN, DCX) and anti-glial (human-specific GFAP, Olig2, or vimentin) antibodies. No neuronal differentiation was seen in any animal and all analyzed GFP+ cells residing in white or gray matter were NeuN or DCX negative (Figure 1I). Analysis of GFP+ cells residing in the white matter (below glia limitans) showed a mixed population of hGFAP, Olig2, APC, and vimentin expressing cells (Figure 3A,C and Figure S5A).

The same immunofluorescence analysis of GFP+ cells residing in the gray matter showed that the majority of GFP+ cells were Olig2 or vimentin positive (Figure 3B and Figure S5B). Only occasional hGFAP+ cells were identified in the gray matter; these hGFAP astrocytes were typically found at the border between the white and gray matter (Figure 3D, inset). Staining with Ki67 (marker of mitotically active cells) antibody showed only occasional presence of GFP/Ki67+ cells in both the white and gray matter (Figure S5F,G). Quantitative analysis of double-stained GFP/Olig2+, GFP/hGFAP+, GFP/Ki67+, and GFP/vimentin+ cells in the white and gray matter is presented in Table 2.

One of the functions of CNS astrocytes is the control of extracellular glutamate concentration. It is mediated by the activity of membrane-bound glutamate transporters (GLAST, GLT1).²² It was demonstrated that the loss or altered function of these transporters can lead to progressive neuronal degeneration (such as seen in ALS) as a result of excessive glutamate receptor activation.^{23,24} To study if the human astrocytes express GLAST, sections were stained with a combination of hGFAP and GLAST antibodies. A highly specific GLAST expression was seen in both the glia limitans-forming human astrocytes as well as in the protoplasmic human astrocytes found in the deeper white matter (Figure 3E-H).

3.4 | Transcriptome analysis of subpially injected NSCs

We next performed mRNA sequencing on the subpially hNSC-injected spinal cord tissue, and used a previously developed bioinformatics method to separate human and rat transcripts from the mixed-species graft¹⁷ (Figure 4A). Using this protocol, the analysis of brain stem,

cervical, thoracic, and lumbar spinal cord revealed the consistent presence of human-specific transcripts (Figure 4B). mRNA transcript analysis demonstrated the preferential upregulation of astrocyte-specific (GFAP, ALDH1L1, AQP4, ALDOC) and oligodendrocyte-specific (MBP, CLDN11) genes, but minimal neuronal transcripts (Figure 4C). In addition, a clear high level expression of SOD1 and LAMB2 (laminin-associated gene) genes was seen (Figure 4D). These results support our observations from immunofluorescence staining, and confirm the preferential differentiation of the grafted hNSCs into glial cells as well as high level of SOD1 protein and human-specific laminin expression in glia limitans-forming human astrocytes. There was no evidence of microglial differentiation in the graft tissue, as microglia do not originate from neural precursors. Furthermore, although NSC genes were still expressed by the grafted cells, there was no evidence of pluripotency-associated gene (NANOG, POU5F1) expression (Figure 4C).

3.5 | Animals injected subpially with hNPCs show normal neurological function and no tumor formation

Assessment of neurological motor function²⁵ showed no detectable changes (such as loss of motor coordination or motor weakness) for the 6-month survival period. Similarly, no presence of allodynia (increased responsiveness after applying normally non-painful stimuli) was seen. Upon spinal cord tissue dissection no macroscopically defined tumor formation or compression-induced neurodegenerative changes were seen in any animals.

4 | DISCUSSION

Using adult rats, we demonstrate potent and widespread spinal and supra-spinal cell migration after the regional subpial delivery of human neural stem cells. Cells that migrated into the white and gray matter differentiated predominately into astrocytes and oligodendrocytes. Robust and functional incorporation of graft-derived astrocytes into the glial limitans was also demonstrated. Because of the simplicity and safety of this approach, our subpial cell delivery technique can potentially be used in future clinical trials testing cell replacement therapies for the treatment of spinal neurodegenerative diseases including ALS, spinal trauma, or transverse myelitis.

4.1 | Mechanisms of cell migration into the spinal parenchyma after subpial cell delivery

The pia mater is the innermost layer of the meninges, and is composed of fibroblasts that ensheath the entire length and surface of the spinal

cord. The glia limitans (glia limiting membrane or lamina limitans) is a thin layer/barrier of GFAP+ astrocytes on the surface of the spinal cord and brain, and is associated with parenchymal basal lamina.^{18,19} Analysis of injected GFP+ cells showed that many of the subpial-injected GFP+ cells effectively incorporated into the glia limitans. In addition, histological-morphological analysis and staining with SOD and human-specific laminin antibodies showed that the hNSC-derived human astrocytes acquired morphological and functional characteristics that are typical of glia limitans-forming endogenous astrocytes. These were characterized by the presence of a high density of human astrocyte-derived foot processes, contributing to the formation of glia limitans, and expression of SOD and synthesis of human-specific laminin, contributing to the formation of the basal membrane. Previous studies have demonstrated that a direct physical contact between pia-forming fibroblast and astrocytes is the primary trigger initiating astrocyte-derived laminin synthesis.²¹ Accordingly, we speculate that a direct interaction of subpially injected hNSCs with the pial membrane is the mechanism leading to laminin synthesis by terminally differentiated hGFAP+ astrocytes. No human-specific laminin was seen in deeper spinal cord or brain tissue. The distribution of GFP+ cells associated with the lamina limitans was found to follow the natural anatomical distribution of lamina limitans, that is, on the surface of the spinal cord and in the penetrating perivascular space.

In addition, a high density of GFP+ cells was found just below the glia limitans as well as in the deep white and gray matter. Based on the injected cell differentiation profile, morphological characteristics and distribution, we speculate that subpially injected multipotent hNSCs enter the deeper spinal parenchyma by active migration across the glia limitans. Some of the migrated GFP+ cells differentiate into GFAP+ astrocytes and functionally incorporate into the glia limitans while other cells, probably still undifferentiated glial precursors, continue to proliferate and migrate into the spinal parenchyma, giving rise to astrocytes and oligodendrocytes found in the deep spinal parenchyma, medulla oblongata, and cerebellum.

4.2 | Preferential glial differentiation of hNSCs after subpial cell delivery

In our current study, the analysis of neuronal vs glial differentiation of injected hNSCs in rats demonstrated a strong preference for glial differentiation (astrocytes and oligodendrocytes), as evidenced by immunostaining, as well as mRNA sequencing analysis. Interestingly, although Olig2 cells derived from injected hNSCs were found in both the white and gray matter throughout the spinal cord, human GFAP+ astrocytes were only present in the lamina limitans and in the deeper white matter, but not in the gray matter. No differentiation toward a neuronal phenotype was observed. In addition, a high density of vimentin-immunoreactive cells as well as occasional presence of Ki67/GFP+ cells were seen throughout the white and gray matter, suggesting the continuing proliferation of glial precursors at 6 months after cell delivery. This is consistent with previous report which demonstrates a continuing proliferation of endogenous glial precursors in non-injured spinal cord in adult mice.²⁶

These data also suggest that the spinal white matter lacks the necessary neuronal induction signals, and further suggests the existence of a highly specific and potent regulatory mechanism which controls astrocyte vs oligodendrocyte differentiation in white vs gray matter. This interpretation is consistent with several previous studies that show a high degree of neuronal differentiation in the core of an hNSC spinal graft targeted to the gray matter, whereas a much higher density of glial cells is observed at the periphery of such grafts.⁵

4.3 | Implications for clinically relevant strategies

The potential future clinical use of a subpial cell delivery technique will be primarily defined by: (a) demonstrated widespread hNSC migration throughout the spinal cord, (b) preferential glial differentiation of multilineage hNSCs upon injection into the subpial space, and (c) the specific spinal neuropathology of the disease to be treated. Several spinal neurodegenerative disorders can be considered. First, the current experimental and clinical cell-replacement therapy to treat ALS employs direct lumbar or cervical gray matter injections of hNSCs.⁹ Because the pathology associated with ALS is widespread and affects motor circuitry throughout the entire spinal cord,⁵ a neuroprotective effect resulting from subpial hNSC grafting could be envisioned by achieving homogeneous cell delivery throughout the spinal cord. In addition, as shown in the present study, the ability to repopulate the lamina limitans by functional SOD and GLAST-expressing astrocytes may lead to additional therapeutic benefits by restoring protective function of the glia limitans and basal membrane (at least in SOD-mutation-caused ALS). Second, one of the concepts in treating traumatic SCI is promoting regional axonal remyelination affected by previous trauma. A current clinical trial (Asterias Inc., Fremont, California) employs human ES-derived OPCs delivered as a single bolus intraparenchymal injection.¹⁰ However, interestingly, experimental data show that axonal demyelination can extend for several segments rostrocaudally after localized SCI, suggesting that a single bolus parenchymal injection of OPCs at the injury epicenter can have only limited remyelination potency at spinal segments distant from the injury site. Thus, adding local subpial delivery of OPCs can lead to accelerated remyelination and more pronounced treatment effect.

Third, the pathology and corresponding neurological dysfunction associated with transverse myelitis is characterized by the loss of local oligodendrocytes and can simultaneously affect multiple segments.^{27,28} Thus, similarly as for spinal trauma, subpial delivery of OPS or hNSCs can be used to restore segmental myelination and function. Fourth, the use of cell-replacement-based therapies for the treatment of lysosomal storage disease by delivering genetically modified cells into the CNS can potentially benefit from the widespread cell repopulation achieved after subpial cell delivery.^{29,30} Finally, there is long lasting interest to employ autologous or allogeneic cells genetically modified to produce antinociceptive inhibitory neurotransmitters such as GABA for the treatment of chronic neuropathic pain.³¹⁻³³ By using a regional subpial injection of such cells, a regionally targeted release of GABA could be achieved and potentially lead to a long lasting, anti-nociceptive effect.

4.4 | Technical requirements to perform effective and safe subpial injection

In our previous studies, we have described the technique of subpial AAV9 vector delivery and identified the pia mater as the major barrier which limits the penetration of the AAV9 vector into the deep spinal parenchyma in mice, rats and pigs.^{12,13} Our original technique used subpial placement of a PE-5 or PE-10 catheter after the pia was punctured using a manually positioned 30G pia-penetrating needle. Our current technique was slightly modified with two XYZ manipulators mounted firmly on a spinal immobilization frame. This modification substantially simplified and improved the safety of the entire subpial cell injection procedure and can readily be used by any surgeon with established expertise to perform spinal laminectomy in rodents, large animal models (pigs, monkeys) or in humans.

ACKNOWLEDGMENTS

We thank Amber Millen for her help with manuscript preparation. K.K., T.T., M.N., S.M., J.C., and M.M. were partially supported by NIH (R01OD018272: M.M.) and SANPORC (M.M.). S.J. and J.J. were supported by the National Sustainability Programme, project number LO1609 (Czech Ministry of Education, Youth and Sports) and RVO: 67985904. H.S. and V.P. were supported by the Czech Science Foundation (Project Number 18-04393S). UCSD Neuroscience Microscopy Facility was supported by NIH (NS047101).

CONFLICT OF INTEREST

Karl Johe and Tom Hazel are employees of and receive salary from Neuralstem, Inc. Martin Marsala is the scientific founder of Neurgain Technologies, Inc. and has an equity interest in the company. In addition, Martin Marsala serves as a consultant to Neurgain Technologies, Inc., and receives compensation for these services. The terms of this arrangement have been reviewed and approved by the University of California, San Diego in accordance with its conflict of interest policies. The other authors indicated no potential conflicts of interest.

AUTHOR CONTRIBUTIONS

K.K., T.T., S.J., J.J., H.S., V.P., S.D., T.G.: carried out or participated in all in vivo work, drafting the manuscript, and the design of the study. M.N.: carried out immunohistochemistry and participated in behavioral assays. T.H., S.M.: carried out cell preparation, shipments, and viability testing before grafting. K.J., S.P., J.C., M.K., M.M.: conceived the study, participated in its design, and drafted the manuscript. All authors read and approved the final manuscript.

DATA AVAILABILITY STATEMENT

All data generated or analyzed during this study are included in this published article (and its supplementary information files).

ORCID

Martin Marsala  <https://orcid.org/0000-0001-5048-6422>

Karl Johe  <https://orcid.org/0000-0002-5967-5868>

REFERENCES

1. Usvald D, Vodicka P, Hlucilova J, et al. Analysis of dosing regimen and reproducibility of intraspinal grafting of human spinal stem cells in immunosuppressed minipigs. *Cell Transplant*. 2010;19:1103-1122.
2. Lu P, Wang Y, Graham L, et al. Long-distance growth and connectivity of neural stem cells after severe spinal cord injury. *Cell*. 2012;150:1264-1273.
3. Lepore AC, Rauck B, Dejea C, et al. Focal transplantation-based astrocyte replacement is neuroprotective in a model of motor neuron disease. *Nat Neurosci*. 2008;11:1294-1301.
4. Gutierrez J, Lamanna JJ, Grin N, et al. Preclinical validation of multi-level intraparenchymal stem cell therapy in the porcine spinal cord. *Neurosurgery*. 2015;77:604-612. discussion 612.
5. Hefferan MP, Galik J, Kakinohana O, et al. Human neural stem cell replacement therapy for amyotrophic lateral sclerosis by spinal transplantation. *PLoS One*. 2012;7:e42614.
6. van Gorp S, Leerink M, Kakinohana O, et al. Amelioration of motor/sensory dysfunction and spasticity in a rat model of acute lumbar spinal cord injury by human neural stem cell transplantation. *Stem Cell Res Ther*. 2013;4:57.
7. Lepore AC, Bakshi A, Swanger SA, Rao MS, Fischer I. Neural precursor cells can be delivered into the injured cervical spinal cord by intrathecal injection at the lumbar cord. *Brain Res*. 2005;1045:206-216.
8. Curtis E, Martin JR, Gabel B, et al. A first-in-human, phase I study of neural stem cell transplantation for chronic spinal cord injury. *Cell Stem Cell*. 2018;22:941-950.e946.
9. Glass JD, Hertzberg VS, Boulis NM, et al. Transplantation of spinal cord-derived neural stem cells for ALS: analysis of phase 1 and 2 trials. *Neurology*. 2016;87:392-400.
10. Priest CA, Manley NC, Denham J, Wirth ED III, Lebkowski JS. Preclinical safety of human embryonic stem cell-derived oligodendrocyte progenitors supporting clinical trials in spinal cord injury. *Regen Med*. 2015;10:939-958.
11. Curtis E, Gabel BC, Marsala M, Ciacci JD. 172 A phase I, open-label, single-site, safety study of human spinal cord-derived neural stem cell transplantation for the treatment of chronic spinal cord injury. *Neurosurgery*. 2016;63(Suppl 1):168-169.
12. Miyahara A, Kamizato K, Juhas S, et al. Potent spinal parenchymal AAV9-mediated gene delivery by subpial injection in adult rats and pigs. *Mol Ther Methods Clin Dev*. 2016;3:16046.
13. Tadokoro T, Miyahara A, Navarro M, et al. Subpial adeno-associated virus 9 (AAV9) vector delivery in adult mice. *J Vis Exp*. 2017;13(125):e55770.
14. Kakinohana O, Cizkova D, Tomori Z, et al. Region-specific cell grafting into cervical and lumbar spinal cord in rat: a qualitative and quantitative stereological study. *Exp Neurol*. 2004;190:122-132.
15. McGinley LM, Sims E, Lunn JS, et al. Human cortical neural stem cells expressing insulin-like growth factor-I: a novel cellular therapy for Alzheimer's disease. *STEM CELLS TRANSLATIONAL MEDICINE*. 2016;5:379-391.
16. Basso DM, Beattie MS, Bresnahan JC. A sensitive and reliable locomotor rating scale for open field testing in rats. *J Neurotrauma*. 1995;12:1-21.
17. Bohaciakova D, Hruska-Plochan M, Tsunemoto R, et al. A scalable solution for isolating human multipotent clinical-grade neural stem cells from ES precursors. *Stem Cell Res Ther*. 2019;10:83.
18. Sofroniew MV. Astrocyte barriers to neurotoxic inflammation. *Nat Rev Neurosci*. 2015;16:249-263.

19. Choi BH. Role of the basement membrane in neurogenesis and repair of injury in the central nervous system. *Microsc Res Tech*. 1994;28:193-203.
20. Peluffo H, Acarin L, Faiz M, Castellano B, Gonzalez B. Cu/Zn superoxide dismutase expression in the postnatal rat brain following an excitotoxic injury. *J Neuroinflammation*. 2005;2:12.
21. Abnet K, Fawcett JW, Dunnett SB. Interactions between meningeal cells and astrocytes in vivo and in vitro. *Brain Res Dev Brain Res*. 1991;59:187-196.
22. Danbolt NC. Glutamate uptake. *Prog Neurobiol*. 2001;65:1-105.
23. Trotti D, Aoki M, Pasinelli P, et al. Amyotrophic lateral sclerosis-linked glutamate transporter mutant has impaired glutamate clearance capacity. *J Biol Chem*. 2001;276:576-582.
24. Maragakis NJ, Rao MS, Llado J, et al. Glial restricted precursors protect against chronic glutamate neurotoxicity of motor neurons in vitro. *Glia*. 2005;50:145-159.
25. Basso DM, Beattie MS, Bresnahan JC. Graded histological and locomotor outcomes after spinal cord contusion using the NYU weight-drop device versus transection. *Exp Neurol*. 1996;139:244-256.
26. Barnabe-Heider F, Goritz C, Sabelstrom H, et al. Origin of new glial cells in intact and injured adult spinal cord. *Cell Stem Cell*. 2010;7:470-482.
27. West TW. Transverse myelitis—a review of the presentation, diagnosis, and initial management. *Discov Med*. 2013;16:167-177.
28. Beh SC, Greenberg BM, Frohman T, Frohman EM. Transverse myelitis. *Neurol Clin*. 2013;31:79-138.
29. Siddiqi F, Wolfe JH. Stem cell therapy for the central nervous system in lysosomal storage diseases. *Hum Gene Ther*. 2016;27:749-757.
30. Kim SU. Lysosomal storage diseases: stem cell-based cell- and gene-therapy. *Cell Transplant*. 2014. <https://doi.org/10.3727/096368914X681946>.
31. Fandel TM, Trivedi A, Nicholas CR, et al. Transplanted human stem cell-derived interneuron precursors mitigate mouse bladder dysfunction and central neuropathic pain after spinal cord injury. *Cell Stem Cell*. 2016;19:544-557.
32. Braz JM, Wang X, Guan Z, et al. Transplant-mediated enhancement of spinal cord GABAergic inhibition reverses paclitaxel-induced mechanical and heat hypersensitivity. *Pain*. 2015;156:1084-1091.
33. Eaton MJ, Berrocal Y, Wolfe SQ. Potential for cell-transplant therapy with human neuronal precursors to treat neuropathic pain in models of PNS and CNS injury: comparison of hNT2.17 and hNT2.19 cell lines. *Pain Res Treat*. 2012;2012:1-31.

SUPPORTING INFORMATION

Additional supporting information may be found online in the Supporting Information section at the end of this article.

How to cite this article: Marsala M, Kamizato K, Tadokoro T, et al. Spinal parenchymal occupation by neural stem cells after subpial delivery in adult immunodeficient rats. *STEM CELLS Transl Med*. 2020;9:177-188. <https://doi.org/10.1002/sctm.19-0156>